Osaka University Knowledge Archive

Title	Ubiquitous Antenna System for Joint Detection of COFDM Signals
Author(s)	Okamura, Shutai; Okada, Minoru; Komaki, Shozo
Citation	IEICE Transactions on Fundamentals of Electronics, Communications and Computer Sciences. 2002, E85-A(7), p. 1685-1692
Version Type	VoR
URL	https://hdl.handle.net/11094/2947
rights	copyright©2008 IEICE
Note	

Osaka University Knowledge Archive : OUKA

https://ir.library.osaka-u.ac.jp/

Osaka University

Institute of Electronics, Information, and Communication Engineers

PAPER Special Section on Multi-dimensional Mobile Information Networks

Ubiquitous Antenna System for Joint Detection of COFDM Signals

Shutai OKAMURA[†a)], *Student Member*, Minoru OKADA[††], *and* Shozo KOMAKI[†], *Regular Members*

SUMMARY In this paper, we propose a new coded orthogonal frequency division multiplex (COFDM)-based ubiquitous antenna system, which is composed of multiple radio base stations (RBSs) deployed over the service area and Radio-on-Fiber (RoF) link that connects RBSs to the central control station (CCS). The proposed system is capable of receiving multiple mobile terminals simultaneously operating at the same frequency by making effective use of joint detection. However, the propagation delay due to the RoF link could be a major problem for realizing the ubiquitous antenna system. In order to overcome this delay problem, we assume that the guard interval of COFDM is longer than the delay difference. Furthermore, in order to improve BER performance in a multipath Rayleigh fading channel, we also propose the MSE normalization scheme followed by the use of an MMSE-based joint detector. Computer simulation results show that the proposed system can improve the frequency utilization efficiency of the broadband wireless access system.

key words: *ubiquitous antenna system, radio-on-fiber, COFDM, joint detection*

1. Introduction

Recently, there have been many research and development activities in wideband wireless local area networks (LANs) in order to establish broadband personal wireless communication networks. In Japan, multimedia mobile access communication systems (MMAC) have been studied by the MMAC Promotion Council [1]. At the MMAC Promotion Council, four wireless communication systems have been standardized as follows: high-speed wireless access, ultrahigh-speed wireless LAN, 5 GHz band mobile access and wireless home link. Particularly, 5 GHz band mobile access has also been standardized as high-speed wireless LAN, known as IEEE802.11a and HIPERLAN/2 [2]. These systems employ orthogonal frequency division multiplex (OFDM) as a physical layer interface. They provide information data rate of up to 54 Mbit/s at an occupied frequency bandwidth of 16.6 MHz. Furthermore, applications of IEEE802.11a and HIPERLAN/2 to public broadband wireless access system are currently being studied as well as wireless LAN application.

However, the bandwidth assigned to the system is not sufficient for deploying radio base stations (RBSs) over the service area. In Japan, frequency bands from 5.15 GHz to 5.25 GHz have been assigned to this 5 GHz wireless LAN system, which accommodates only four physical frequency channels in a 100 MHz band. This makes the frequency allocation for each RBS difficult when many RBSs are deployed.

We have previously proposed a ubiquitous antenna system, which is composed of multiple microcell RBSs deployed over the service area and Radio-on-Fiber (RoF) link that connects RBSs to the central control station (CCS) [3], [4]. Figure 1 illustrates a ubiquitous antenna system. All the RBSs are deployed over the service area at 100-m intervals and connected to the CCS with RoF link. In this system, the signals transmitted from mobile terminals (MTs) are propagated through multipath channels and received by the plural of the RBSs. The received radio frequency (RF) signal by each RBS is input to an electrical-to-optical (E/O) converter to modulate the intensity of the optical carrier and the modulated optical signal is sent to the CCS via RoF link. At the CCS, all optical signals from the RBSs are converted to RF signals again by the corresponding optical-to-electrical (O/E) converters. Then, the CCS performs all the demodulation sequences and signal processing. Since all the received signals at the RBSs are collected to the CCS, we can employ more sophisticated signal processing techniques

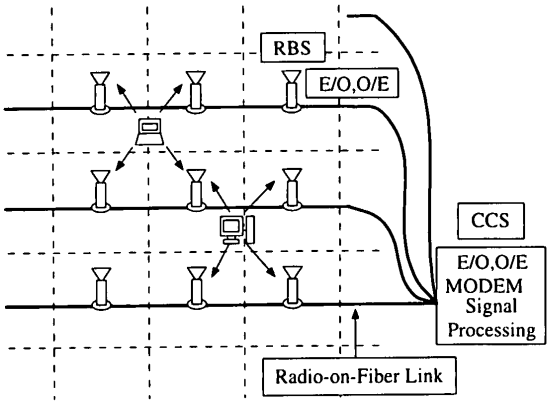

Fig. 1 Ubiquitous antenna system.

Manuscript received October 26, 2001.
Manuscript revised February 7, 2002.
Final manuscript received March 20, 2002.

[†]The authors are with the Department of Communications Engineering, Faculty of Engineering, Osaka University, Suita-shi, 565-0871 Japan.
[††]The author is with the Graduate School of Information Science, Nara Institute of Science and Technology, Ikoma-shi, 630-0101 Japan.
a) E-mail: okamura@roms.comm.eng.osaka-u.ac.jp

NII-Electronic Library Service

Institute of Electronics, Information, and Communication Engineers

such as interference cancellation and joint detection at the CCS. The proposed ubiquitous antenna system enables the multiple MT to operate at the same frequency channel simultaneously by making effective use of joint detection. Therefore, the proposed system can improve the frequency utilization efficiency of broadband wireless access systems. Furthermore, since the RBS performs only E/O and O/E conversion, we can not only reduce hardware complexity and cost of the RBS but also share the RBS with variable wireless services. By this, we can create an open frequency wireless network that is not dependent on the frequency band and the air interface, and flexibility of the radio resource utilization is improved.

Clark et al. also proposed an alternative antenna array system whose antenna elements are distributed over the service area and array signal processing is performed in the central server connected to each array element by analog link [5]. They indicated that the distributed antenna array system has threefold capacity gain compared with the conventional centralized one. However, in the above systems, since the distance between any two RBSs is around one hundred meters, about several hundred nanoseconds delay difference due to RoF link has been detected. Therefore, it is difficult to realize the system. In [4] and [5], the propagation delay due to RoF link and multipath propagation has not been taken into account.

In this paper, we propose a new coded OFDM (COFDM)-based ubiquitous antenna system. COFDM is one of the multicarrier transmission techniques that are capable of transmitting broadband signals in heavy multipath environments. To set the guard interval of COFDM signals such that it be longer than the delay difference, the proposed system can mitigate the effects of the delay difference due to RoF link and effectively perform the joint detection [6]–[8]. As a joint detector, we employ the minimum mean square error (MMSE) based algorithm as described in the next Sect. [9]. Furthermore, in order to improve the gain of frequency diversity by the error correction coding of COFDM signals, we also propose a new joint detection scheme that includes a normalization component. In the proposed scheme, the output of the joint detector is normalized by the mean square error (MSE). As a result, it provides us to obtain the implicit subcarrier diversity effect after the forward error correction (FEC). Then, we apply the ubiquitous antenna system to 5 GHz Wireless LANs and show that the proposed system can improve the frequency utilization efficiency compared with conventional systems.

The rest of this paper is organized as follows. Section 2 illustrates the proposed ubiquitous antenna system. In Sect. 3, we analyze the BER performance and the frequency utilization efficiency by computer simulation and show the superiority of the proposed system from the results of computer simulations. Finally, conclusions are given in Sect. 4.

2. Ubiquitous Antennas for COFDM

2.1 System Model

In this section, we describe the proposed ubiquitous antenna system based joint detector. The system model considered in this paper is illustrated in Fig. 2. Suppose that M MTs in the service area transmit COFDM signals simultaneously at the same frequency channel. We assume that the entire bandwidth of COFDM signal is divided into K subcarriers. At m-th MT, the binary

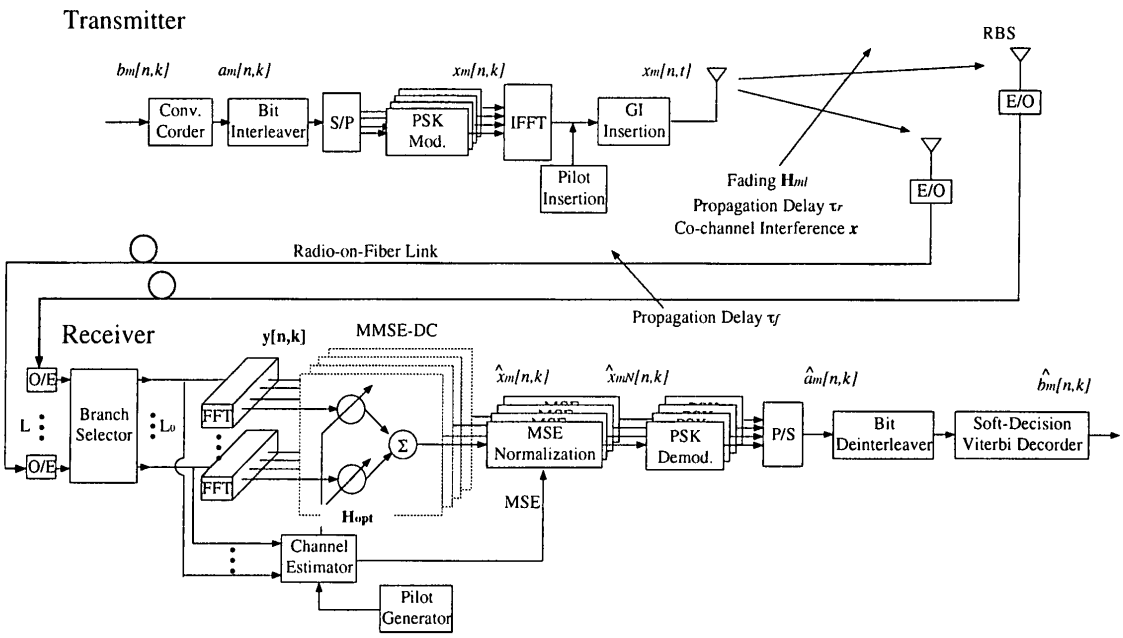

Fig. 2 System model of the proposed ubiquitous antenna system.

NII-Electronic Library Service

Institute of Electronics, Information, and Communication Engineers

bit stream $b_m[n,k]$ of the n-th symbol is coded into $a_m[n,k]$'s across each COFDM subcarrier using convolutional error correction coding. $a_m[n,k]$'s are interleaved and then modulated into $x_m[n,k]$'s using phase shift keying (PSK) modulation. In order to estimate the channel impulse response (CIR) between each MT and each RBS, the transmitter inserts pilot symbols before information data symbols. $x_m[n,k]$'s are then modulated into multicarrier signals $x_m[n,t]$'s by an inverse fast Fourier transform (IFFT) processor. The guard interval, also known as the cyclic extension, is inserted in order to remove the inter-symbol interference (ISI) due to delay spread. After that, the signal is transmitted to the RBSs through the radio propagation channel.

In a radio propagation path, the signal transmitted from each MT is affected by fading, co-channel interference, propagation delay and path loss. The signals are received by the L RBSs. The received signal at each RBS is disrupted by the additive white Gaussian noise (AWGN), converted to optical signal by an E/O converter, and sent to the CCS via the RoF link. In the RoF link, the signals are distorted by optical link noise and non-linear distortion, and delayed. At the CCS, the O/E converters convert the optical signals from RBSs to electrical signals again. For notational convenience, we omit the indices $[n,k]$ and define the $L \times 1$ received signals vector $\mathbf{y} = [y_1, y_2, \ldots, y_L]^T$ by

$$\mathbf{y} = \mathbf{H}\mathbf{x} + \mathbf{z}, \tag{1}$$

where the $M \times 1$ vector $\mathbf{x}$ of transmitted signals and the $L \times 1$ AWGN vector $\mathbf{z}$, zero mean and variance σ_n^2, respectively, are given by

$$\mathbf{x} = [x_1, x_2, \ldots, x_M]^T, \tag{2}$$

$$\mathbf{z} = [z_1, z_2, \ldots, z_L]^T, \tag{3}$$

where $\mathbf{x}^T$ denotes the transpose of $\mathbf{x}$. The frequency response matrix $\mathbf{H}$ of dimension $L \times M$ is constituted by the set of $L \times 1$ frequency response vectors of the M MTs,

$$\mathbf{H} = (\mathbf{H}_1, \mathbf{H}_2, \ldots, \mathbf{H}_M), \tag{4}$$

where $\mathbf{H}_m$ is given by

$$\mathbf{H}_m = [H_{m1}, H_{m2}, \ldots, H_{mL}]^T, \tag{5}$$

where H_{ml} is the frequency response between m-th MT and l-th RBS at the corresponding symbol and subcarrier. In this paper, we assume that H_{ml}'s for different m's of l's are independent, stationary, and complex Gaussian with zero mean.

2.2 Channel Estimation

In order to perform the joint detection, the estimation of CIR is required at the receiver. In the proposed system, each MT inserts the pilot symbol that satisfies the optimum MSE condition discussed in [10], [11]. It is given by

$$x_m[0,k] = x_1[0,k] W_K^{K_0 mk}, \tag{6}$$

where $W_K = \exp(-j2\pi/K)$ is the complex Fourier kernel, and K_0 denotes the largest integer smaller than or equal to K/M.

The receiver estimates the CIR by calculating the correlation between the received signal at each RBS and the reference pilot signal, and the estimated CIR is given by

$$h_{ml}[\tau] = \frac{1}{K} \sum_{t=0}^{K_0} x_m[0,t] y_l[0, t+\tau]. \tag{7}$$

Then, the receiver obtains $H_{ml}[n,k]$ by applying $h_{ml}[t]$ into the FFT processor.

2.3 Joint Detection

As the joint detector, we employ an MMSE-diversity combiner (DC). The MMSC-DC is an optimum linear receiver in terms of minimizing the MSE. When the receiver has perfect knowledge of channel response $\mathbf{H}$, the MMSE-DC minimizes the error even if a large number of branches are used. On the other hand, when there is an estimation error in the channel response used in MMSE-DC, the MMSE-DC is no longer optimum. MSE at the output of the receiver increases with increasing number of branches, particularly in the low E_b/N_0 region, or in the case of a large estimation error in channel response. In order to solve this problem, the receiver chooses the L_0 signals that have larger desired signal power than the remaining $L - L_0$ signals. We define the corresponding $L_0 \times 1$ received signal vector and the $L_0 \times M$ frequency response matrix as $\mathbf{y}_0$ and $\mathbf{H}_0$, respectively.

Before the MMSE-DC, the received signal from each RBS is divided into each subcarrier by the corresponding FFT processor. Then, the MMSE-DC is performed on the subcarrier by subcarrier basis. The $M \times L_0$ optimum weight matrix $\mathbf{H}_{opt}$ is given by

$$\mathbf{H}_{opt} = \mathbf{H}_0{}^H \mathbf{R}_{yy}^{-1}, \tag{8}$$

where $\mathbf{R}_{yy}$ is $L_0 \times L_0$ correlation matrix of $\mathbf{y}_0$ and defined by

$$\begin{aligned} \mathbf{R}_{yy} &\triangleq E_c[\mathbf{y}_0 \mathbf{y}_0{}^H] \\ &= \mathbf{R}_s + \mathbf{R}_n, \quad \text{with} \\ \mathbf{R}_s &= \mathbf{H}_0 \mathbf{H}_0{}^H \\ \mathbf{R}_n &= \sigma_n^2 \mathbf{I}, \end{aligned} \tag{9}$$

where E_C is the conditional expectation. $\mathbf{I}$ and $\mathbf{x}^H$ denote an $L_0 \times L_0$ identity matrix and the Hermitian transpose of $\mathbf{x}$, respectively. The output of the MMSE-DC is given by

$$\hat{\mathbf{x}} = \mathbf{H}_{opt} \mathbf{y}_0. \tag{10}$$

$\hat{\mathbf{x}}$ is the estimated transmitted signal vector.

NII-Electronic Library Service

Institute of Electronics, Information, and Communication Engineers

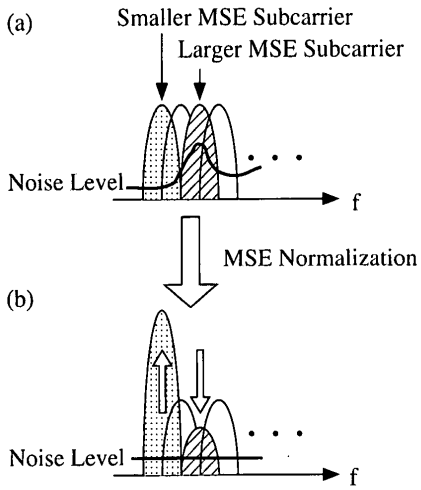

Fig. 3 The proposed MSE normalization.

2.4 MSE Normalization

Figure 3(a) shows the desired signal and noise power at the output of MMSE-DC. All the sub-channels have the same desired signal power while the noise power at each sub-channel differs from those of other channels. On the other hand, the following Viterbi decoder uses the Euclidean distance as path metrics, that is, the decoder is optimum in terms of minimizing the bit error rate when all the noises are independent and identically distributed (i.i.d.) Gaussian random variables. In order to make the Viterbi decoder optimum, the output signal of MMSE-DC is normalized by MSE or the noise variance of the corresponding signal. The MSE for m-th MT is given by

$$MSE_m = \sigma_d^2 - \mathbf{H}_m^H \mathbf{R}_{yy}^{-1} \mathbf{H}_m, \tag{11}$$

where σ_d is the desired signal power [12]. This normalization is performed on a subcarrier by subcarrier basis as well as the MMSE-DC. The output of MSE normalizer for m-th MT, $\hat{x}_{mN}$, is given by

$$\hat{x}_{mN} = \hat{x}_m / MSE_m. \tag{12}$$

The noise at the output of the MSE normalization is i.i.d., as shown in Fig. 3(b), and the Viterbi decoder shows optimum performance. We will show this diversity effect by computer simulation in the next section.

Then, the normalized signals are demodulated, deinterleaved and applied to the soft-decision Viterbi decoder. Finally, we can obtain the desired user's binary bit streams $\hat{b}_m[n,k]$.

3. Numerical Results

In this section, we analyze the performance of the proposed ubiquitous antenna based wireless LAN system by computer simulation. In the following, we evaluate BER performance and frequency utilization efficiency in up-link.

Table 1 COFDM signal configurations.

Modulation	QPSK-OFDM
FFT Size	64
Number of Subcarriers	48
Symbol Duration	4.2 μs
Guard Interval	1 μs
Data Length	10 symbols
Pilot Symbol Length	1 symbol
FEC	Convolution Constraint Length=6 Code Rate=1/2
Channel	Equal Gain 2-ray Rayleigh Fading Channel
Interval between Two Rays	150 ns
RoF Link Delay	500 ns at Cell Size of 100 m
Path Loss Exponent	4.0

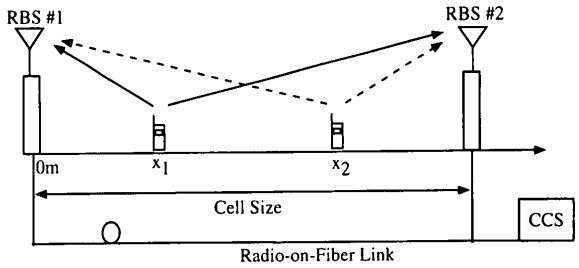

Fig. 4 The allocation of RBSs for BER analysis.

The COFDM signal configurations used in our simulation are shown in Table 1. They are modified 5 GHz wireless LAN standards to suit the proposed system. As subcarrier modulation format, we assume quadrature phase shift keying (QPSK) with coherent detection. The initial phase is estimated by using pilot tones attached to the beginning of the packet. As propagation channel, equal gain two-ray Rayleigh fading channel is assumed. The interval between two rays is 150 ns. The path loss exponent is 4.0. We also assume that the symbol timing of the COFDM signals is synchronized at every MT. The signals are sent to the RBSs through propagation channels. In the following, the propagation delay due to wireless channel is taken into account. We ignore the frequency offset between MTs and CCS local oscillators, and the non-linear distortion due to RoF link.

3.1 BER Performance of the Proposed System

3.1.1 BER Performance vs. E_b/N_0

Firstly, in order to show the basic property of the proposed system, we analyze the BER performance of the proposed system. The simulation model is shown in Fig. 4. We assume that two RBSs are deployed along the horizontal axis and there are two MTs in the service area. Each RBS is connected to the CCS by RoF link. The distance between the first RBS and the k-th MT is given by x_k, where $k = 1$ and 2. In the pro-

NII-Electronic Library Service

Institute of Electronics, Information, and Communication Engineers

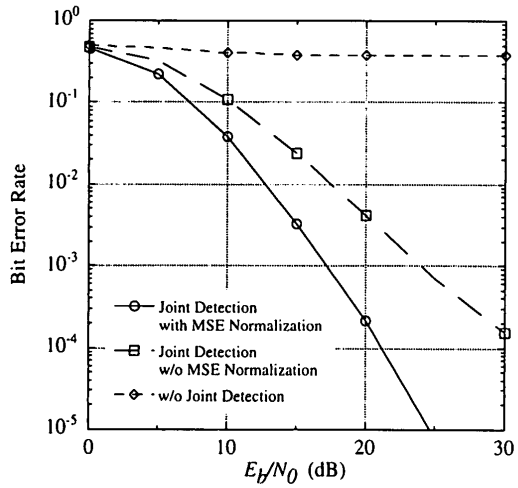

Fig. 5 BER performance of the proposed MMSE-based joint detector with/without MSE normalization in an equal gain two-sample spaced two-ray Rayleigh fading channel. We assume two MTs and two RBSs, $x_1 = 50\,\mathrm{m}$, $x_2 = 50\,\mathrm{m}$, and cell size is 100 m. Desired-to-undesired signal power ratio is 0 dB.

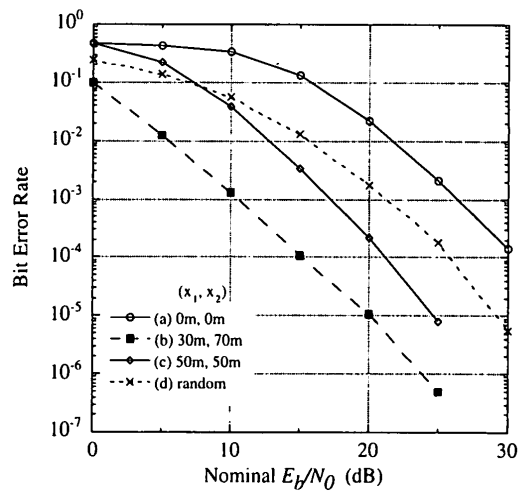

Fig. 6 BER performance of the proposed system with MSE normalization vs. nominal E_b/N_0 at a cell size of 100 m in a two-ray Rayleigh fading channel. (a) $x_1 = 0\,\mathrm{m}$, $x_2 = 0\,\mathrm{m}$, (b) $x_1 = 30\,\mathrm{m}$, $x_2 = 70\,\mathrm{m}$, (c) $x_1 = 50\,\mathrm{m}$, $x_2 = 50\,\mathrm{m}$, (d) each of them is chosen randomly.

posed system, the propagation delay due to both radio propagation path and RoF link and the path loss are dependent on the position of MT (x_k) and cell size.

In order to show the effect of the proposed MSE normalization scheme, the BER performance of the proposed joint detector with/without MSE normalization is shown in Fig. 5. In this simulation, we assume a cell size of 100 m, which causes 500 ns delay in RoF link. The positions of MTs are $x_1 = 50\,\mathrm{m}$ and $x_2 = 50\,\mathrm{m}$, which mean that the received desired-to-undesired signal power ratio is 0 dB. From Fig. 5, we can see that MSE normalization gives a power gain of 8 dB at BER=10^{-3} by making effective use of the implicit subcarrier diversity effect.

In order to evaluate the performance in various situations, we consider four situations for the position of MTs, (a) $x_1 = 0\,\mathrm{m}$, $x_2 = 0\,\mathrm{m}$, (b) $x_1 = 30\,\mathrm{m}$, $x_2 = 70\,\mathrm{m}$, (c) $x_1 = 50\,\mathrm{m}$, $x_2 = 50\,\mathrm{m}$ and (d) the position of each MT is chosen randomly. BER performance vs. nominal E_b/N_0 at a cell size of 100 m is shown in Fig. 6. The nominal E_b/N_0 is the E_b/N_0 when MT is located at the center of two RBSs. In case (a), since the two MTs are positioned very closely and the difference in received signal power between two RBSs is large, the gain of MMSE-DC is small. Hence, the performance is the worst. On the other hand, the results for case (c) are better. In this case, although the two MTs are positioned closely, the CCS can perform joint detection since the two RBSs obtain sufficient signal power to perform the joint detection. We obtain the best performance, in case (b), because the distance between the two MTs is large implying that the interference signal power is small. The result of case (d) represents the average BER taking into account various MT positions. BER performance in this case is worse than those in cases (b) and (c). However, it achieves

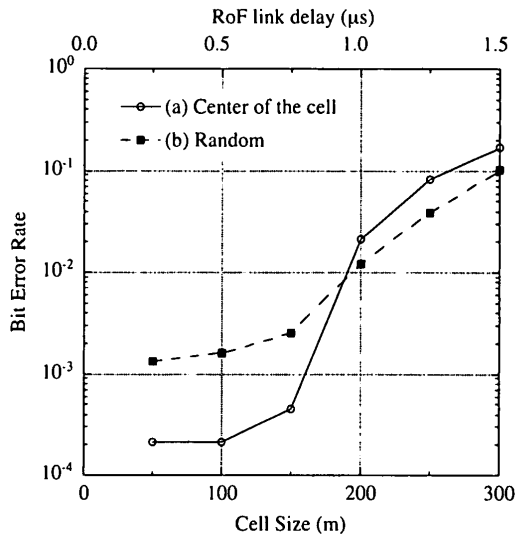

Fig. 7 BER performance of the proposed system with MSE normalization vs. cell size at $E_b/N_0 = 20\,\mathrm{dB}$ and in the two-ray Rayleigh fading channel. (a) Both MTs are at the center of the cell and (b) the position of each MT is chosen randomly.

relatively high BER performance, lower than 10^{-5} at nominal $E_b/N_0 = 30\,\mathrm{dB}$.

3.1.2 BER Performance vs. Cell Size

In the above simulation, the delay spread due to both RoF link and radio propagation path is shorter than the guard interval of COFDM signals. However, the delay spread would exceed the guard interval in a larger cell size region. Hence, in order to evaluate the effect of the delay spread exceeding the guard interval on the performance of the joint detection, we plot BER performance vs. cell size at nominal $E_b/N_0 = 20\,\mathrm{dB}$ in Fig. 7. In this simulation, we also consider two situations regarding MT position: (a) both MTs are at the center of the

NII-Electronic Library Service

Institute of Electronics, Information, and Communication Engineers

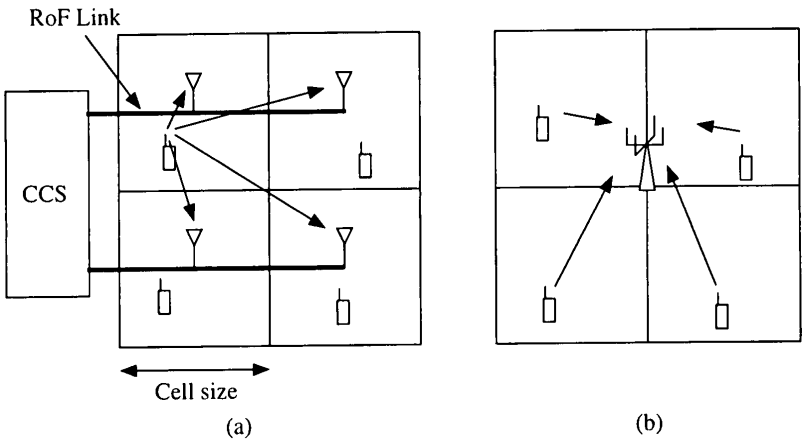

Fig. 8 The allocation of RBSs for frequency utilization efficiency analysis. (a) The proposed ubiquitous antenna system; (b) the central antenna system.

cell, (b) the position of each MT is chosen randomly.

From Fig. 7, when cell size exceeds 200 m, BER becomes worse because the delay spread due to both RoF link and radio propagation path exceeds the guard interval of COFDM signals. Hence, in order to obtain the sufficient performance for providing wireless LANs, we have to manage the delay, cell size and guard interval.

3.2 Frequency Utilization Efficiency of the Proposed System

Next, we analyze the frequency utilization efficiency of the proposed system. The allocation of the RBSs in order to cover the service area is shown in Fig. 8. We assume four RBSs throughout the analysis. In the proposed ubiquitous antenna system shown in Fig. 8(a), the service area is divided into four cells and one RBS is located at the center of each cell. All the RBSs are connected to the CCS by the RoF link, and the CCS performs the MMSE-DC-based joint detection. All the MTs transmit COFDM signals simultaneously at the same frequency channel. For comparison, we evaluate the performance of a ubiquitous antenna system without joint detection. In this case, all the RBSs have their own demodulators and each RBS demodulates the received signals independent of the other RBSs. All the MTs are still operating at the same frequency, similar to the proposed system. Furthermore, we evaluate the macro-cell system, or one RBS is located at the center of the service area. In the following, we call it the central antenna system. We assume the central antenna system with and without joint detection. In the case of joint detection, the RBS has an array antennas and MMSE-DC-based joint detection is performed using the array antenna. In the central antenna system without joint detection, however, the RBS has only one antenna element and no joint detection is performed. Similar to the case of the ubiquitous antenna system, all the MTs are operating at the same frequency simultaneously. Moreover, we also evaluate a conventional digital communication system in which all the MTs are accessing the RBS located the center of the macro-cell and equipped only with one antenna elements, in time division multiple access (TDMA) mode. In all cases, all the MTs are uniformly distributed over the service area. In this simulation, we assume that the data rate is 11.5 Mbps at an occupied frequency bandwidth of 15 MHz and the transmission is successful when there is no bit error in a packet composed of a pilot symbol and ten information symbols.

3.2.1 Frequency Utilization Efficiency vs. E_b/N_0

First, we evaluate the frequency utilization efficiency of the proposed ubiquitous antenna system vs. E_b/N_0. The transmission power of an MT is determined so that E_b/N_0 per unit branch equals nominal E_b/N_0 at one RBS antenna that is 70 m apart from the corresponding MT. Figure 9 shows the frequency utilization efficiency per unit cell vs. nominal E_b/N_0 at a cell size of 100 m. In case of the conventional system and the central antenna system without joint detection, the frequency utilization efficiency is about 0.1 bits/s/Hz. On the other hand, applying the ubiquitous antenna system improves the frequency utilization efficiency up to 0.4 bits/s/Hz. Furthermore, upon applying the joint detection to the ubiquitous and central antenna systems, both systems show improved the frequency utilization efficiency. Especially in the lower nominal E_b/N_0 region, the frequency utilization efficiency of the ubiquitous antenna system is higher, about 60%, than that of the central one. Hence, the proposed system enables low power transmission and improves not only the frequency utilization efficiency but also the power efficiency.

3.2.2 Frequency Utilization Efficiency vs. Cell Size

Next, similar to Sect. 3.1.2, we also analyze the effect of the delay spread exceeding the guard interval on the frequency utilization efficiency. Figure 10 shows the fre-

NII-Electronic Library Service

Institute of Electronics, Information, and Communication Engineers

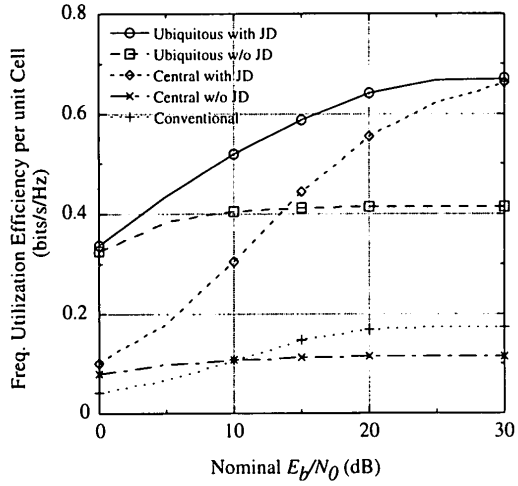

Fig. 9 Frequency utilization efficiency per unit cell of the proposed system vs. nominal E_b/N_0 at a cell size of 100 m. "JD" means joint detection. 4 MTs; 4RBSs; uniformly distributed terminals; two-ray Rayleigh fading channel.

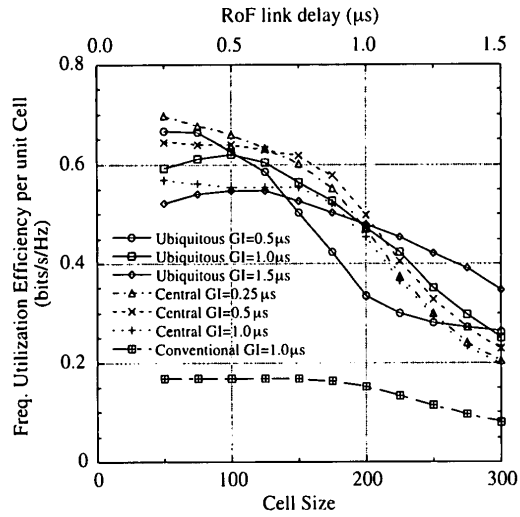

Fig. 10 Frequency utilization efficiency per unit cell of the proposed system vs. cell size at $E_b/N_0 = 20$ dB. 4 MTs; 4RBSs; uniformly distributed terminals; two-ray Rayleigh fading channel.

quency utilization efficiency per unit cell vs. cell size at nominal $E_b/N_0 = 20$ dB. Applying the joint detection to the ubiquitous and central antenna systems, we can obtain higher frequency utilization efficiency than that of the conventional one. The shorter the guard interval is, the higher the frequency utilization efficiency is in a small cell size region. This is because the guard interval increases the bandwidth. On the other hand, the longer the guard interval is, the higher the frequency utilization efficiency is in a large cell size region, since the guard interval mitigates BER performance degradation due to delay spread that becomes large in a larger cell size region. Again, the use of a long guard interval reduces the frequency utilization efficiency, that is, the frequency utilization efficiency becomes worse with increasing cell size even if the proper guard interval is chosen. Fortunately, the delay difference due to RoF link can be managed by adjusting the fiber length. Therefore, we could further improve the performance of the ubiquitous antenna system in a large cell size region by managing the delay.

4. Conclusions

In this paper, we have proposed a new COFDM-based ubiquitous antenna system that is capable of receiving multiple MTs simultaneously operating at the same frequency. The system employs MMSE-based joint detection algorithm. In order to improve the bit error rate performance in a multipath Rayleigh fading channel, we have also proposed the MSE normalization scheme that normalizes the outputs of the MMSE-based joint detector by MSE. Computer simulation results show that the proposed ubiquitous antenna system improves the frequency utilization efficiency compared with the conventional microcellular system despite the propagation delay difference in the RoF link.

Acknowledgement

This research was partially supported by the Japan Society for the Promotion of Science, Grant-in-Aid for Encouragement of Young Scientists (A) 13750350, 2001.

References

[1] ARIB, "What is MMAC," http://www.arib.or.jp/mmac/e/what.html

[2] R. van Nee, G. Awater, M. Morikura, H. Takanashi, M. Webster, and K.W. Halford, "New high-rate wireless LAN standards," IEEE Commun. Mag., vol.37, no.12, pp.82–88, Dec. 1999.

[3] S. Komaki, K. Tsukamoto, M. Okada, and H. Harada, "Proposal of radio highway networks for future multimedia-personal wireless communications," ICPWC'94, pp.204–208, Bangalore, India, Aug. 1994.

[4] M. Toyama, M. Okada, and S. Komaki, "Maximal ratio combining macro diversity for micro-cellular slotted ALOHA," IEICE Trans. Commun. (Japanese Edition), vol.J79-B-I, no.5, pp.271–277, May 1996.

[5] M.V. Clark, T.M. Willis, L.J. Greenstein, A.J. Rustako, Jr., V. Erceg, and R.S. Roman, "Distributed versus centralized arrays in broadband wireless networks," Proc. Vehicular Technology Conference, MA1-2, Rhodes, Greece, May 2001.

[6] S. Okamura, M. Okada, and S. Komaki, "Interference cancellation for COFDM systems based on ubiquitous antennas," Proc. 2000 Communications Society Conference of IEICE, B-5-136, p.424, Oct. 2000.

[7] S. Okamura, M. Okada, and S. Komaki, "Multi-user detection of COFDM signals using ubiquitous antennas," IEICE Technical Report, RCS 2000-161, Nov. 2000.

[8] S. Okamura, M. Okada, and S. Komaki, "Impact of ubiquitous antennas to the interference cancellation of COFDM systems," Proc. 6th International OFDM-Workshop (InOWo'01), 2-1, Sept. 2001.

[9] Y. Li and R. Sollenberger, "Adaptive antenna arrays for OFDM systems with cochannel interference," IEEE Trans. Commun., vol.47, no.2, pp.217–229, Feb. 1999.

NII-Electronic Library Service

Institute of Electronics, Information, and Communication Engineers

[10] Y. Li, N. Seshadri, and S. Ariyavisitakul, "Channel estimation for OFDM systems with transmitter diversity in mobile wireless channels," IEEE J. Sel. Areas Commun., vol.17, no.3, pp.461–471, March 1999.
[11] M. Mümster and L. Hanzo, "Improved decision-directed channel estimation for multi-user OFDM environments," Proc. Vehicular Technology Conference, Rhodes, Greece, May 2001.
[12] S. Haykins, Adaptive Filter Theory, 3rd Edition, Prentice-Hall, 1996.

Shutai Okamura was born in Kochi, Japan, in 1977. He received the B.E. degree in electrical and electronic engineering from Shizuoka University, in 2000, and the M.E. degree in Communications Engineering from Osaka University, in 2001. He is currently pursuing the Ph.D. degree at Osaka University, and engaging in the research on radio communication systems.

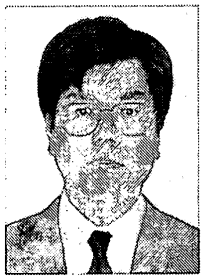

Minoru Okada received the B.E. degree in communications engineering from the University of Electro-Communications, Tokyo, Japan, in 1990 and the M.E. and Ph.D. degrees both in communications engineering from Osaka University, Osaka, Japan, in 1992 and 1998, respectively. Since 1993, he was with the Department of Communications Engineering, Osaka University, as a Research Associate. From 1999 to 2000, he was with the University of Southampton, U.K., as a Visiting Research Fellow. In 2000, he joined the Graduate School of Information Science, Nara Institute of Science and Technology, Nara, Japan, where he is currently an Associate Professor. Dr. Okada is a member of IEICE, the Institute of Electrical and Electronics Engineers (IEEE), and the Institute of Image Information and Television Engineers of Japan (ITE). He received the Young Engineer Award from IEICE in 1999.

Shozo Komaki was born in Osaka, Japan, in 1947. He received B.E., M.E. and Ph.D. degrees in Electrical Communication Engineering from Osaka University, in 1970, 1972 and 1983 respectively. In 1972, he joined the NTT Radio Communication Labs., where he was engaged in repeater development for a 20-GHz digital radio system, 16-QAM and 256-QAM systems. From 1990, he moved to Osaka University, Faculty of Engineering, and engaging in the research on radio and optical communication systems. He is currently a Professor of Osaka University. Dr. Komaki is a senior member of IEEE, and a member of the Institute of Television Engineers of Japan(ITE). He was awarded the Paper Award and the Achievement Award of IEICE, Japan in 1977 and 1994 respectively.

NII-Electronic Library Service